Superconductivity in transparent zinc-doped In₂O₃ films having low carrier density

Kazumasa Makise[1], Nobuhito Kokubo[2], Satoshi Takada[3], Takashi Yamaguti[3], Syunsuke Ogura[3], Kazumasa Yamada[3], Bunjyu Shinozaki[3], Koki Yano[4], Kazuyoshi Inoue[4] and Hiroaki Nakamura[4]

[1] High Voltage Electron Microscopy Station, National Institute for Material Science,
3–13 Sakura, Tsukuba, Ibaraki 305-3003, Japan
[2] Center for Research and Advancement in Higher Education, Kyushu University,
Fukuoka 810-8560, Japan
[3] Department of Physics, Faculty of Sciences, Kyushu University, Fukuoka 810-8560, Japan
[4] Advanced Technology Research Laboratories, Idemitsu Kosan Co. Ltd, Chiba 299-0293,
Japan

E-mail: Makise.kazumasa@nims.go.jp

Abstract

Thin polycrystalline zinc-doped indium oxide (In₂O₃–ZnO) films were prepared by post-annealing amorphous films with various weight concentrations x of ZnO in the range $0 \leqslant x \leqslant 0.06$. We have studied the dependences of the resistivity ρ and Hall coefficient on temperature T and magnetic field H in the range $0.5 \leqslant T \leqslant 300$ K, $H \leqslant 6$ T for 350 nm films annealed in air. Films with $0 \leqslant x \leqslant 0.03$ show the superconducting resistive transition. The transition temperature T_c is below 3.3 K and the carrier density n is about 10^{25}–10^{26} m^{-3}. The annealed In₂O₃–ZnO films were examined by transmission electron microscopy and x-ray diffraction analysis revealing that the crystallinity of the films depends on the annealing time. We studied the upper critical magnetic field $H_{c2}(T)$ for the film with $x = 0.01$. From the slope of dH_{c2}/dT, we obtain the coherence length $\xi(0) \approx 10$ nm at $T = 0$ K and a coefficient of electronic heat capacity that is small compared with those of other oxide materials.

Keywords: transparent thin films, carrier density, electrical resistivity, annealing effect, superconductivity

(Some figures in this article are in colour only in the electronic version)

1. Introduction

Transparent electrode materials, such as In₂O₃ and tin-doped indium oxide (ITO), are well known and are already used in devices such as liquid crystal displays. Recently, amorphous indium zinc oxide (a-In₂O₃–ZnO) films have attracted considerable practical interest, because these films can give a smooth surface, which enables detailed processing with a high accuracy, and have large values of Hall mobility compared with a-In₂O₃ films. Some characteristics have been investigated, such as electrical resistivity [1] and the effect of the substrate temperature on the mobility and morphology [2] in a-In₂O₃–ZnO films. However, detailed studies of the transport properties at low temperatures are few. The electrical

properties of a-In_2O_3–ZnO are very interesting from the viewpoint of quantum corrections in dirty systems with low carrier densities.

Recently, for a-In_2O_3–ZnO films, we have examined the electrical properties in the temperature range of $2 < T < 300$ K [3]. For films with thickness $d = 350$ nm and weight concentration of ZnO $x \sim 0.1$, the temperature dependence of the resistivity $\rho(T)$ shows metallic characteristics, that is, $d\rho/dT > 0$, in a wide temperature range. However, we did not observe superconductivity in this temperature range. Although post-annealing in a vacuum does not increase the resistivity, annealing in air brings about a large resistivity change owing to the reduction of the carrier density n. Therefore we can consider that the free carriers are supplied by oxygen deficiency as well as by substitutional Zn. Concerning the effect of post-annealing in air on films with $x = 0.1$, it is reported that films annealed at 300 °C for 1 h have an amorphous structure [4]. However, for films with $x < 0.1$, it is expected that the annealing effect in air improves the material properties. Indeed, annealing at 250–450 °C increases the resistivity and optical transparency of ITO films [5]. The resistivity increase is associated with decreasing mobility. Higher transparency is important for optical applications; it was attributed to the improved crystallinity of the films. As for the appearance of superconductivity, Mori [6] reported that ITO films attain a sharp superconducting transition by proper annealing and found that annealing at a relatively low temperature results in superconductivity. Recently, the superconductor-insulator transition in amorphous films of high carrier-density indium-oxide has been studied by Kowal and Ovadyahu [7]. They reported that In_xO films with $n < 10^{26}$ m^{-3} do not show superconductivity. Carrier density can be controlled by adjusting the annealing conditions; the new oxide material with lower carrier density than that observed up to now is expected to show superconductivity. For the purpose of finding a new type of superconductor with low carrier density, In_2O_3–ZnO is a suitable material.

In this work, we report superconductivity in In_2O_3–ZnO films prepared under certain annealing conditions. To clarify the occurrence of superconductivity, we have investigated the film structure by x-ray diffraction (XRD) analysis and high-resolution transmission electron microscopy (HRTEM). Further, we used electron energy-loss spectroscopy (EELS) in a TEM (TEM–EELS) to find the relationship between the transport characteristics and the micro- and nanostructure of the present materials.

2. Film preparation and experimental procedures

First, a-In_2O_3–ZnO films with $d = 350$ nm were prepared by dc-magnetron sputtering on glass substrates using the ceramic oxide In_2O_3–ZnO target under 0.3 Pa of Ar. We prepared several targets with different weight concentrations x of ZnO, $x = 0.0, 0.005, 0.01, 0.02, 0.03, 0.04, 0.05$ and 0.06. During deposition, the substrate was kept at room temperature. XRD reveals that these as-grown films have amorphous structure. The properties of In oxide films

(structure, resistivity, etc) strongly depend on the deposition conditions. In particular, polycrystalline ITO films have been deposited without post-annealing by reactive magnetron sputtering [8]. Although these films show metallic behavior, that is, $d\rho/dT > 0$, in a wide temperature range, films show not superconductivity but insulating behaviors owing to localization or electron–electron effects at temperatures below 50 K.

We measured the temperature T and magnetic field H dependence of resistance $R(T, H)$ by a standard dc four-probe technique. We applied H up to 6 T perpendicular to the film surface. Data on Hall coefficients R_H were obtained in a standard manner. The photoresist lift-off method was used to obtain the necessary adequate pattern for Hall voltage. To eliminate the effect of Hall probe misalignment, measurements were performed in both positive and negative magnetic configurations. The results were averaged over the two perpendicular field orientations. For the Hall resistance, we confirmed that a linear dependence holds up to above $H = \pm 5$ T. Electrical transport properties of resistivity ρ, carrier density n and mobility μ were measured from 0.5 to 300 K.

After deposition, we annealed the films in air. As the annealing temperature T_a, we adopted 200 and 300 °C. We annealed the films for a duration t_a from 0.5 to 48 h by putting the glass substrate on a heated plate kept at a constant temperature within 0.5 K.

3. Experimental results and discussion

Figure 1 shows the $\rho(T)$ dependence at some external magnetic fields perpendicular to the surface of the film with $x = 0.005$ annealed at 300 °C for 2 h. The resistivity shows a drastic decrease at around 2 K, indicating the superconducting transition. We recognize the decrease of T_c by applying the external magnetic field. The inset shows $\rho(T)$ at $H = 0$ and 5 T in a wide temperature range. Large negative magnetoresistivity is observed in a normal state temperature range. Figure 1(b) shows detailed data of the negative magnetoresistivity of the present In oxide systems at some temperatures near the onset of the superconductivity for In_2O_3 with $x = 0$ annealed at 300 °C for 2 h in N_2 atmosphere. The superconducting transition temperature is around 0.5 K. Magnetoresistivity $\Delta\rho$, defined as $\Delta\rho = [\rho(H) - \rho(0)]/\rho(0)$, initially increases owing to the destruction of superconductivity with increasing magnetic field. In stronger magnetic fields, $\Delta\rho$ becomes maximum at a certain value of H_m. At temperatures $T < 2$ K and fields $H < 5$ T, $\Delta\rho$ is positive in spite of $d(\Delta\rho)/dH < 0$ at high fields. The value of H_m decreases with increasing temperature. At temperatures above 2.5 K, $\Delta\rho$ becomes negative at $H > 2$ T. Finally, at temperatures > 6 K, $\Delta\rho$ becomes negative for any magnetic field. Although the positive $\Delta\rho$ at low fields and low temperatures mainly results from the destruction of superconductivity by the magnetic field, the quantum correction due to the electron localization and electron–electron interactions in dirty systems will give a dominant contribution to $\Delta\rho$ in a stronger magnetic field and at higher temperatures. In the case of weak spin
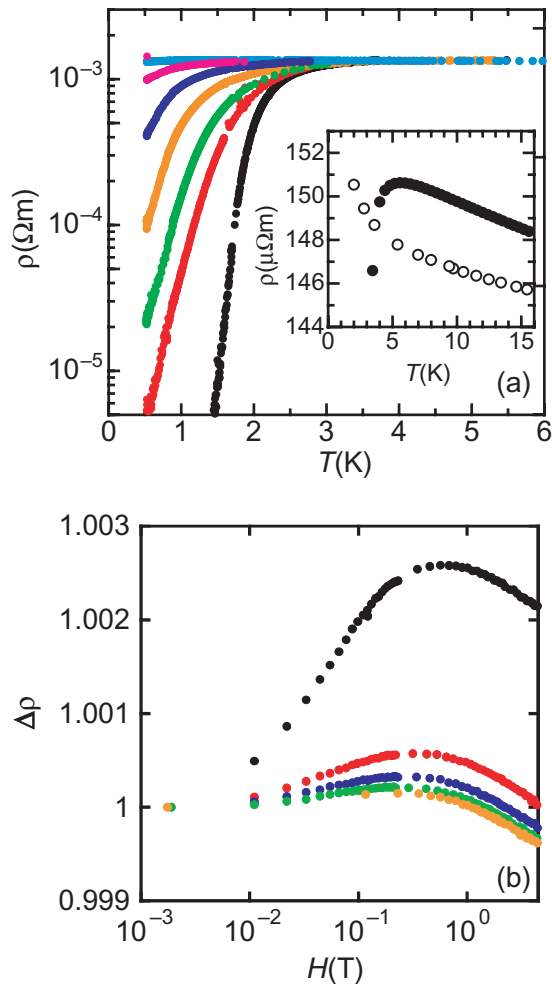
Figure 1. (a) T dependence of ρ of polycrystalline In$_2$O$_3$–ZnO film with weight concentration of ZnO $x = 0.005$ in various magnetic fields perpendicular to the film surface: $H = 0, 0.1, 0.3, 1.0, 2.0, 3.0$, and 4.0 T. The film was prepared by annealing as-grown amorphous In$_2$O$_3$–ZnO at 300 °C for 2 h. The inset shows the detailed data near the onset of superconducting transition at $H = 0 (\bullet)$ and $H = 5$ T$(\circ)$. (b) Normalized magnetoresistivity defined as $\Delta\rho = [\rho(H) - \rho(0)]/\rho(0)$ at temperatures $T = 1.5, 2, 2.5, 3$ and 3.5 K from top to bottom.

orbit scattering, the correction brings about the negative magnetoresistivity. Such a negative $\Delta\rho$ in transparent oxide materials has been investigated in two- and three-dimensional a-In$_2$O$_3$–ZnO films [3]. Then, the present results of $\Delta\rho$ are explained by the competition in the destructions of superconductivity and localization (and/or electron–electron interaction) by the magnetic field.

Figure 2(a) shows the cross-sectional high angle annular dark-field scanning transmission electron microscopy (HAADF–STEM) image of the film with $x = 0.005$ annealed at 300 °C for 2 h. A cross-sectional TEM sample was prepared by a focused ion beam method. We can see the large grains separated by boundaries in the central part of the image. Figures 2(b) and (c) show the intensities of HAADF–STEM and EELS O-K edge line profile, respectively. These data were taken along the solid line of length ≈ 50 nm across the grain boundary in figure 2(a). The position indicated by the arrow in figure 2(b) corresponds to the crossing point with
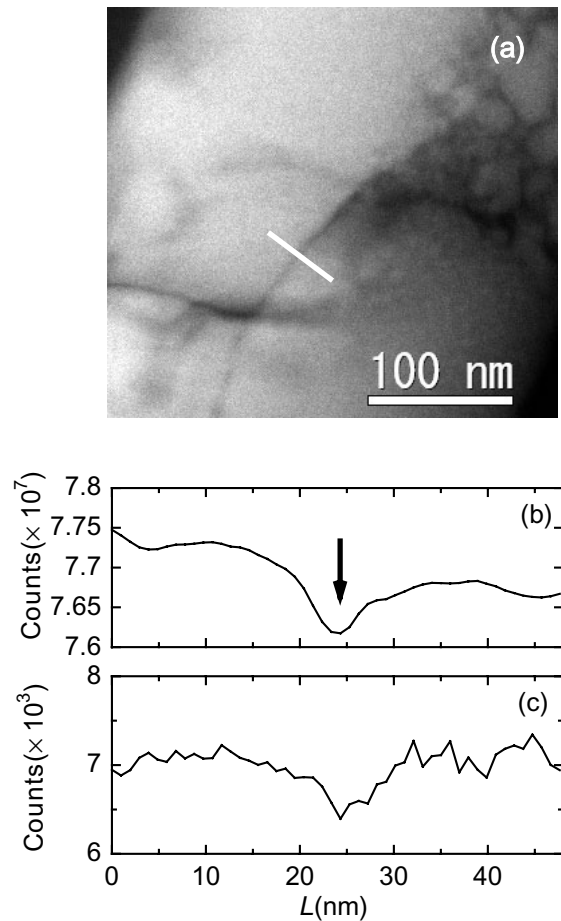
Figure 2. (a) Cross-sectional HAADF-STEM image of grains and grain boundaries of In$_2$O$_3$–ZnO film with $x = 0.05$. (b) Intensity of HAADF–STEM and (c) EELS O-K edges. Line shows the profile taken on thick line crossing the grain boundary in HAADF–STEM image in (a). The point indicated by the arrow corresponds to the grain boundary.

the grain boundary. The experimental result that the shapes of the line profiles in figures 2(b) and (c) are almost the same suggests that neither oxygen nor In aggregate at the grain boundary. As shown in figure 1(a), crystallized In$_2$O$_3$–ZnO films annealed at $T_a = 300$ °C show superconductivity. The transition temperature of films annealed at 300 °C lies between 0.5 and 2.0 K depending on the concentration x of ZnO. However, the value of T_c does not show a systematic change depending on x or annealing time t_a, as far as the annealing temperature is chosen as $T_a = 300$ °C. On the contrary, films annealed at $T_a = 200$ °C show a systematic change of T_c depending on x and t_a; the resistivity and transition temperature T_c monotonically increase with increasing t_a for the investigated films with $x = 0.005, 0.01$ and 0.02.

Figure 3(a) shows XRD patterns of films with $x = 0.01$ annealed at 200 °C for five different t_a. The indexes correspond to the bixbite structure of In$_2$O$_3$ [9]. It is found that the diffraction peak height increases with t_a. In order to quantify the effect of annealing time on the crystallinity, we introduce a factor P from the analyses of the height of the XRD patterns as follows. Figure 3(b) shows the t_a dependence
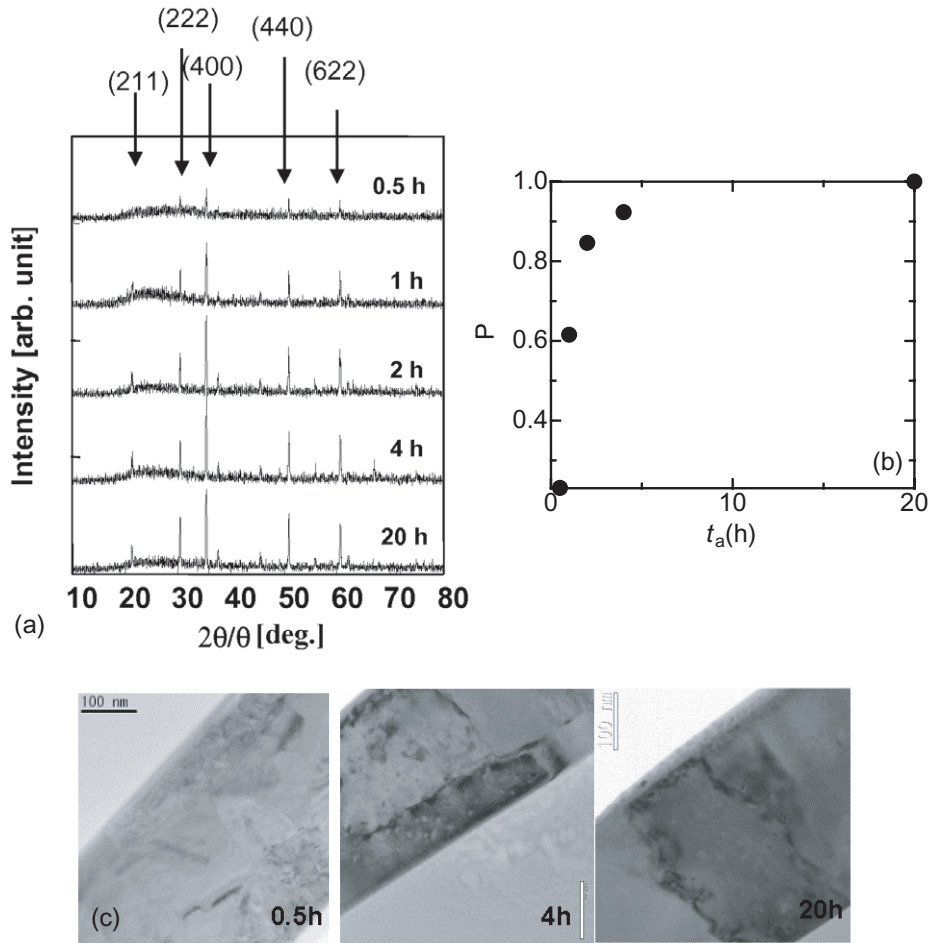
Figure 3. (a) XRD pattern of films annealed at 200 °C for different annealing times t_a. (b) t_a dependence of crystallinity factor P defined as $P(t_a) = \sum P_i(t_a)/\sum P_i(t_a = 20\,\text{h})$. The quantity $P_i(t_a)$ corresponds to the peak height of diffractions (211), (222), (400), (440) and (622) for a film annealed for duration t_a. (c) TEM images for films annealed at 200 °C for 0.5, 4.0 and 20 h.

of $P(t_a)$, which is defined by

$$P(t_a) = \sum P_i(t_a)\Big/ \sum P_i(t_a = 20\,\text{h}), \qquad (1)$$

where each $P_i(t_a)$ corresponds to the peak height of diffraction (211), (222), (400), (440) and (622) for the film annealed for t_a. We observe crystallization even for the film annealed for only 0.5 h. The quantity P increases sharply for $0.5 < t_a < 2$ h and seems to saturate with $t_a > 4$ h. Figure 3(c) shows the TEM images for films annealed at 200 °C. As t_a increases, the grain size increases. This finding is consistent with data shown in figures 3(a) and (b).

Figure 4(a) shows the $\rho\text{–}T$ curves for films with different values of t_a, where the data on a-In$_2$O$_3$–ZnO ($t_a = 0$) film are also included. The resistivity ρ increases with increasing t_a. Although the films annealed for 20 and 48 h show the insulating characteristic with $\mathrm{d}\rho/\mathrm{d}T < 0$, other films show metallic behavior throughout the whole temperature range. All films, except a-In$_2$O$_3$–ZnO, exhibit the superconducting transition, as shown in figure 4(b).

Figure 5(a) presents the t_a dependence of T_c and carrier density n for films with $x = 0.01$ annealed at 200 °C. Although both T_c and n change drastically for short t_a and apparently saturate with long t_a, the two quantities show completely opposing behaviors. By annealing at 200 °C for several hours, carrier density n changes by about one-tenth. When we compare the carrier densities of the present films to those of previous materials showing superconductivity, the estimates in this work are smaller by a factor of 10–100. The mobility μ increases from 20 to 50 cm^2 Vs^{-1} with t_a increasing from 0 (amorphous film) to 4 h. Further increase of t_a results in a gradual decrease of μ.

We cannot explain this reverse behavior on the basis of the Bardeen–Cooper–Schrieffer theory, in which T_c is given by $T_c = 1.13\Theta_D\exp(-1/gN_F)$, where Θ_D, g and N_F are the Debye temperature, the coupling constant and the density of states at Fermi energy, respectively, if we assume constant g and the free electron model. As mentioned above, there is a possibility that the change in the crystal structure brings about superconductivity. Therefore, it is necessary to further study the crystal structure of each film annealed at different t_a to further investigate the superconductivity.

From the t_a dependences of P and T_c given in figures 3(b) and 5(a) for films with $x = 0.01$ annealed at 200 °C, we speculate on the effect of crystallization on T_c. Figure 5(b) shows the P dependence of normalized T_c, where P is defined in equation (1). The monotonic increase of T_c suggests that
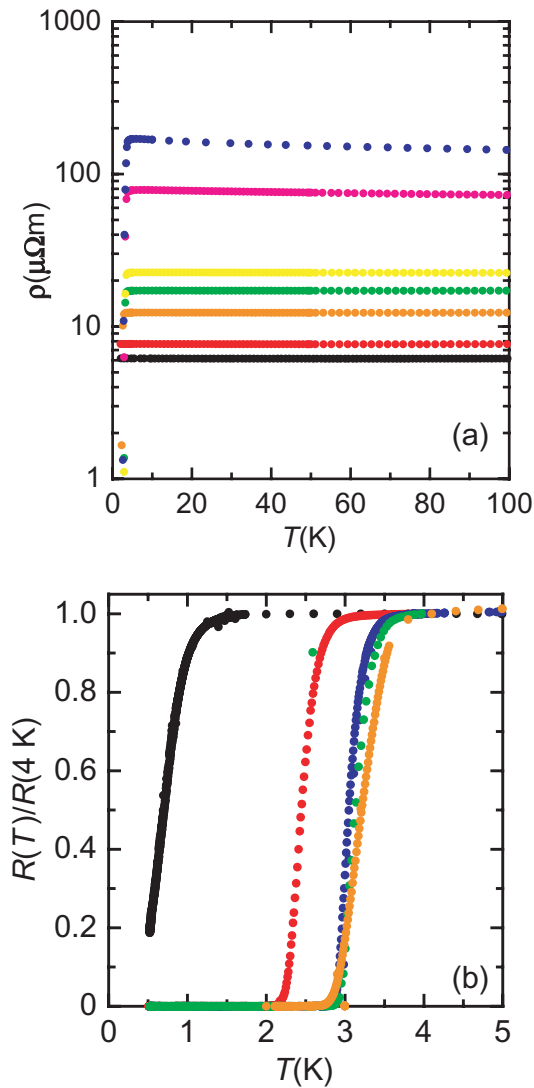
Figure 4. (a) $\rho(T)$ dependence for films with $x = 0.01$ annealed at 200 °C for 0 (amorphous), 0.5, 1.0, 2.0, 4.0, 20 and 48 h from bottom to top. (b) Normalized resistance $R(T)/R(T = 4.2\,\text{K})$ for five films annealed for 0.5, 1.0, 2.0, 4.0 and 20 h from left to right.

superconductivity of the present oxide films is dominated by the crystal structure and/or crystallinity for films annealed at 200 °C.

Using the data in figure 5(a), we show the n dependence of T_c in figure 6 not only for films with $x = 0.01$ but also for films with $x = 0.005$ and 0.02. Within experimental error, T_c of our In oxide films is equal to or less than T_c of pure In metal ($\sim 3.4\,\text{K}$). However, our critical magnetic fields are much higher than those of pure In ($\leqslant 0.03\,\text{T}$). Therefore, superconductivity in our In oxide films cannot be assigned to metallic In channels. A similar decrease in T_c with carrier density was observed for In nitride films [10]. In InN, the critical temperature decreases with carrier density n not only at high, but also at low n of approximately $4 \times 10^{23}\,\text{m}^{-3}$. The low-density decrease is associated with the Mott transition and it should be observed in In oxide films as well; it could not be verified in the present study because of the insufficiently low carrier density in our films. Although the exact value
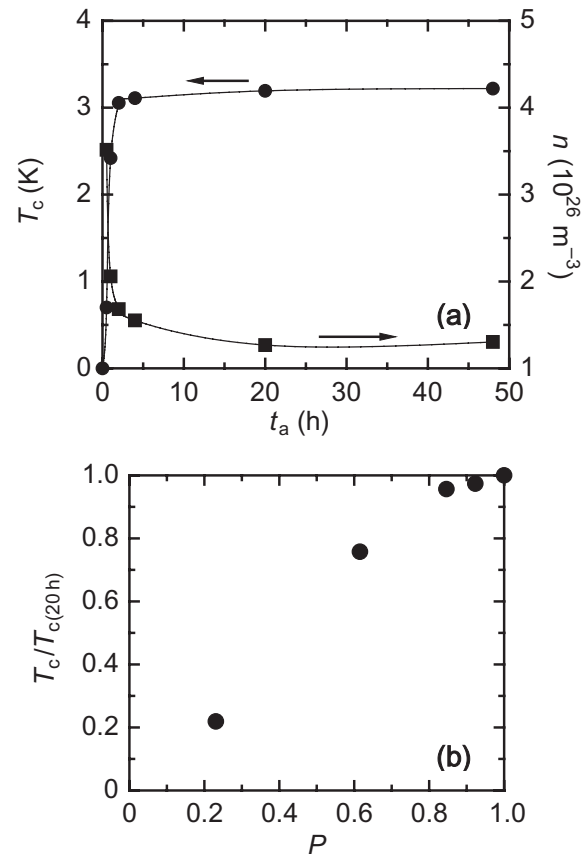

Figure 5. (a) Dependences of T_c (●) and n (■) on annealing time t_a for films with $x = 0.01$. The value of T_c was defined as the temperature at which half of the normal-state resistance was restored. (b) Dependence of T_c on crystallinity factor P.
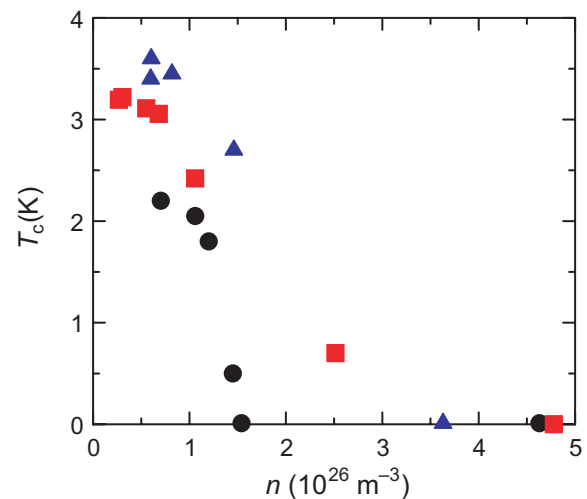

Figure 6. Dependence of T_c on carrier concentration n for films with $x = 0.005$(●), $x = 0.01$(■) and $x = 0.02$(▲) annealed at 200 °C. The symbols on the horizontal axis are data of as-grown amorphous films.

of T_c depends on x, the qualitative characteristics of $T_c(n)$ are almost the same for three groups with different values of $x = 0.005$, 0.01 and 0.02. The value of T_c seems to increase as x increases for $x \leqslant 0.02$ in the present work. However, it is expected that T_c will become maximum and then decrease
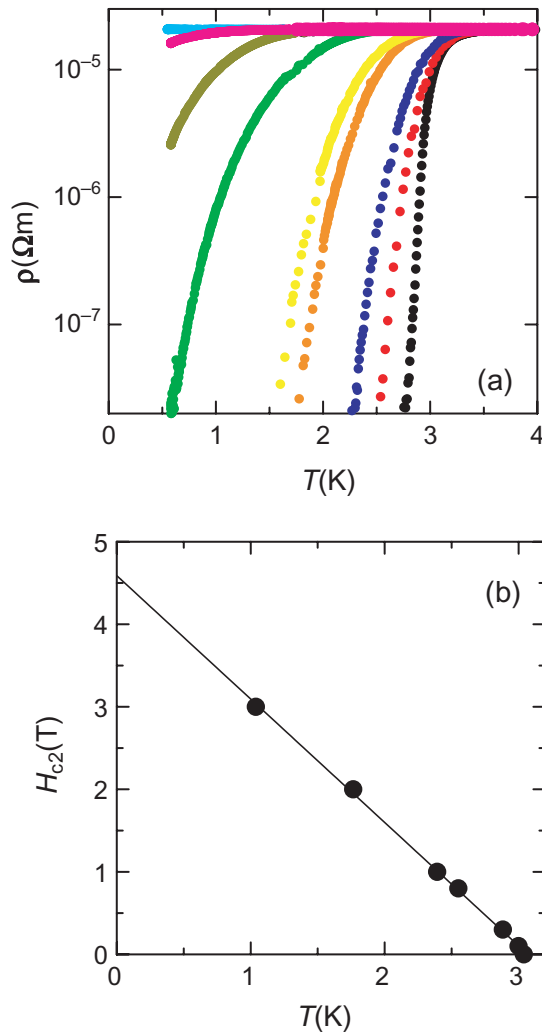
Figure 7. (a) T dependence of ρ of In$_2$O$_3$–ZnO with $x = 0.01$ annealed at 200 °C for 2 h at magnetic fields $H = 0$, 0.1, 0.3, 0.8, 1.0, 2.0, 3.0, 4.0 and 6.0 T. (b) T dependence of the upper critical magnetic field H_{c2}.

as x increases further, because the films annealed at 300 °C do not show superconductivity for $x > 0.03$, as mentioned in the previous section.

Figure 7(a) shows the typical $\rho(T)$ dependence at various magnetic fields for the film with $x = 0.02$ annealed at 200 °C for 2 h. Figure 7(b) shows the temperature dependence of the upper critical magnetic field H_{c2}. According to the Ginzburg–Landau theory, the coherence length $\xi(0)$ is given by

$$\xi(0) = \{\phi_0/2\pi T_c |(\mathrm{d}H_{c2}/\mathrm{d}T)_{T\approx T_c}|\}^{-1/2}, \qquad (2)$$

where ϕ_0 is the flux quantum ($\phi_0 = hc/2\mathrm{e} = 2.07 \times 10^{-15}$ Wb). From the value of $|\mathrm{d}H_{c2}/\mathrm{d}T|$ determined in figure 7(b) and the above relation, we obtain the length $\xi(0) \approx 10$ nm. Using the free electron model and the formula $|(\mathrm{d}H_{c2}/\mathrm{d}T)_{T\approx T_c}| = 4k_{\mathrm{B}}/\pi\mathrm{e}D$, where D is the diffusion constant and k_{B} is the Boltzmann constant, we can also obtain

the following relation for the coefficient of the electronic heat capacity γ as follows [11],

$$\gamma = 2.23 \times 10^{-4}\sigma_n |(\mathrm{d}H_{c2}/\mathrm{d}T)_{T\approx T_c}|, \qquad (3)$$

where σ_n is the normal-state conductivity. For the present film, $\gamma \approx 20$ has been obtained using values of σ_n and $|(\mathrm{d}H_{c2}/\mathrm{d}T)_{T\approx T_c}|$. This value is small compared with that of pure In, $\gamma \approx 110$. This finding is consistent with the low carrier density of the film, $n \sim 8 \times 10^{25}$ m^{-3}.

4. Conclusions

We have prepared polycrystalline In$_2$O$_3$–ZnO films from as-grown amorphous films by annealing in air, and observed superconductivity at temperatures below 3.3 K for films with restricted values x of the weight concentration of ZnO. EELS indicated no segregation of In at the grain boundaries. The critical temperature T_c and carrier concentration n of films with $x = 0.01$ annealed at 200 °C change systematically with annealing time. XRD patterns and the dependence of T_c on annealing time t_a suggest that T_c correlates with the crystallinity.

From the slope of $\mathrm{d}H_{c2}/\mathrm{d}T$ and the conductivity of films with $x = 0.01$ annealed at 200 °C we have obtained the coherence length of $\xi(0) \approx 10$ nm at $T = 0$ K and a small coefficient of the electronic heat capacity compared with that of other oxide materials.

Acknowledgment

References

[1] Minami T, Kasumu T and Takata S 1996 *J. Vac. Sci. Technol.* A **14** 1704
[2] Jung Y S, Seo J Y, Lee D W and Jeon D Y 2003 *Thin Solid Films* **445** 63
[3] Shinozaki B, Makise K, Shimane Y, Nakamura H and Inoue K 2007 *J. Phys. Soc. Japan* **76** 074718
[4] Sasabayashi T, Ito N, Nishimura E, Kon M, Song P K, Utumi K, Kaijo A and Shigesato Y 2003 *Thin Solid Films* **445** 219
[5] Mohamed H A and Ali H M 2008 *Sci. Technol. Adv. Mater.* **9** 025026
[6] Mori N 1993 *J. Appl. Phys.* **73** 1327
[7] Kowal D and Ovadyahu Z 2008 *Physica* C **4** 322
[8] Ohno S, Kawaguti Y, Miyahara A, Sato Y, Song P K, Yoshikawa M, Frach P and Shigesato Y 2006 *Sci. Technol. Adv. Mater.* **7** 56
[9] Yaglioglu B, Huang Y J, Yeom Y H and Paine D C 2006 *Thin Solid Film* **496** 89
[10] Inushima T 2006 *Sci. Technol. Adv. Mater.* **7** S112
[11] Saint-James D, Sarma G and Thomas E J 1969 *Type II Superconductivity (International series of monographs in Nature Philosophy* vol 19) ed T Haar (Oxford: Pergamon) p 174